Numerical investigation on the mode coupling contact dynamic instabilities.

Jacopo Brunetti, Francesco Massi, Walter d'Ambrogio, Yves Berthier

Numerical investigation on the mode coupling contact dynamic instabilities.

Jacopo Brunetti[1, 2], Francesco Massi[1, 3], Walter D'Ambrogio[2], Yves Berthier[1]
[1] *Université de Lyon, CNRS, INSA-Lyon, LaMCoS UMR 5259, 20 Rue Des Sciences, 69621, Villeurbanne, France*
E-mail: jacopo.brunetti@insa-lyon.fr

[2] *Università dell'Aquila, Dipartimento di Ingegneria Industriale e dell'Informazione e di Economia, Via G. Gronchi, 18, 67100, L'Aquila (AQ), Italy*

[3] *Università di Roma La Sapienza, Dip. di Ingegneria Meccanica e Aerospaziale, via Eudossiana, 18, 00184, Roma, Italy*

Keywords: Frictional Contact, Mode Coupling Instability, Unstable Induced Vibration.

SUMMARY.
In complex mechanical systems the frictional contact is at the origin of significant changes in the dynamic behavior. Unstable vibrations can reach large amplitude that could compromise the integrity of the systems and are often associated with annoying noise emissions. In this paper the numerical analysis of a lumped system constituted by several degrees of freedom in frictional contact with a slider is presented, where the introduction of friction gives rise to an unstable dynamic behavior. Two different approaches are used to investigate the effects of frictional forces: i) a linear Complex Eigenvalue Analysis (CEA) allows for calculating the complex eigenvalues of the system that can be characterized by a positive real part (i.e. negative apparent modal damping); ii) a non linear model has been developed that accounts for the non linear behavior at the contact interface (stick, slip, detachment) to solve the time history solution and analyze the unstable vibrations.

1 INTRODUCTION

Complex mechanical systems under frictional contact are always subjected to vibrations induced by the frictional contact. Such vibrations can be either of low amplitude, due to the system response at the broadband noise excited at the contact surface, or characterized by an unstable response of the system dynamics (stick-slip, sprag-slip, mode lock-in) and their consequent large amplitude. The presence of frictional contact can give rise to mode-coupling instabilities that produce harmonic "fiction induced vibrations". Unstable vibrations can reach large amplitude that are often associated with annoying noise emission.

The study of this kind of contact dynamic instability has been subject of many numerical [1],[2] and experimental [3] studies on specific mechanical systems, such as automotive brakes, typically affected by such issue. These works have shown how the stable and unstable behavior of the system can be identified by a Complex Modal Analysis (CEA) and that the frequency found to be unstable both experimentally and numerically is close to one of the unstable modes resulting form the CEA. Theoretic and numerical analyses of simple lumped models considered mainly systems with no more than one unstable mode to observe the effect of some parameters on the complex eigenvalues of the system [4] or on size of the limit cycle of oscillations [5]. Often, contact non linearities have been replaced by non linear stiffness in order to apply non linear resolution methods [4]. By the analysis of the contact behavior of complex mechanical systems it can be observed that the variation of contact

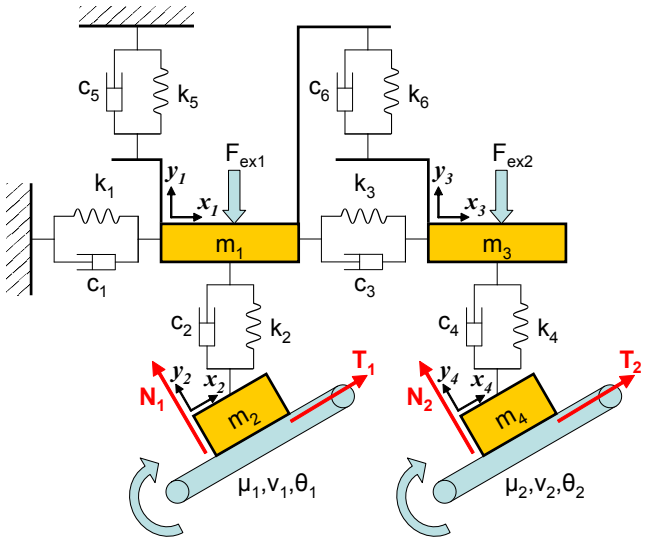

Figure 1: Lumped system considerd for calculations.

status strongly affects the limit cycle; periodical variations of contact status can be found locally at the contact [6], affecting the maximum amplitude of vibration reached by the mechanical system (limit cycle).

In this paper, the numerical analysis of a lumped system constituted by several degrees of freedom in frictional contact with a slider is presented, where the introduction of friction can give rise to an unstable dynamic behavior. The non linear effects of the contact are in this case accounted for by considering the possibility of switching between sliding, sticking and detachment of the bodies in contact. Two approaches are used to investigate the effects of friction forces. The CEA allows for calculating the complex eigenvalues of the system that can be characterized by positive real part (i.e. negative apparent modal damping). The effects of the main parameters on the system stability are investigated. In the second approach, a non linear model has been developed to account for the real contact behavior at the interface to calculate the transient solution and analyze the unstable vibrations. The transient response of the system is directly related to the results from the CEA.

2 LUMPED MODEL

The analyzed system is composed by 4 masses m_i, where 2 masses are in contact with rigid sliders with a constant friction coefficient μ (Fig. 1). The sliders are inclined at the angle θ_i and move with speed $v_{p,i}$.

The two masses belonging to the same vertical line are constrained to have the same horizontal position. External forces $F_{ex,1}$ and $F_{ex,2}$ applied to the upper masses m_1 and m_3 ensure a preload at the contact. The contact between the sliders and the lower masses m_2 and m_4 acts as an unilateral

constraint ($y_2 \geq 0$ e $y_4 \geq 0$) and the reaction forces can be expressed as follow:

$$\begin{cases} N_1 \neq 0,\ T_1 \leq -\mu \dfrac{\dot{x}_2 - v_p}{\|\dot{x}_2 - v_p\|} N_1 & \text{if } y_2 = 0 \\ N_2 \neq 0,\ T_2 \leq -\mu \dfrac{\dot{x}_4 - v_p}{\|\dot{x}_4 - v_p\|} N_2 & \text{if } y_4 = 0 \\ N_1 = 0,\ T_1 = 0 & \text{if } y_2 > 0 \\ N_2 = 0,\ T_2 = 0 & \text{if } y_4 > 0 \end{cases} \tag{1}$$

Referring to the DoFs introduced in Fig.1, the equations of motion of the system can be expressed as follows:

$$\begin{cases} -m_1\ddot{x}_1 - c_1\dot{x}_1 + c_3(\dot{x}_3 - \dot{x}_1) - k_1x_1 + k_3(x_3 - x_1) = F_1 \\ -m_1\ddot{y}_1 - c_2(\dot{y}_1 - \dot{x}_2\ \sin\theta_1 - \dot{y}_2\ \cos\theta_1) - c_5\dot{y}_1 + c_6(\dot{y}_3 - \dot{y}_1) \\ \quad -k_2(y_1 - x_2\sin\theta_1 - y_2\cos\theta_1) - k_5y_1 + k_6(y_3 - y_1) = Fex, 1 \\ -m_2\ddot{x}_2 + c_2(\dot{y}_1 - \dot{x}_2\sin\theta_1 - \dot{y}_2\cos\theta_1)\sin\theta_1 \\ \quad +k_2(y_1 - x_2\sin\theta_1 - y_2\cos\theta_1)\sin\theta_1 = -F_1\cos\theta_1 - T_1 \\ -m_2\ddot{y}_2 + c_2(\dot{y}_1 - \dot{x}_2\sin\theta_1 - \dot{y}_2\cos\theta_1)\cos\theta_1 \\ \quad +k_2(y_1 - x_2\sin\theta_1 - y_2\cos\theta_1)\cos\theta_1 = F_1\sin\theta_1 - N_1 \\ -m_3\ddot{x}_3 - c_3(\dot{x}_3 - \dot{x}_1) - k_3(x_3 - x_1) = F_2 \\ -m_3\ddot{y}_3 - c_4(\dot{y}_3 - \dot{x}_4\sin\theta_2 - \dot{y}_4\cos\theta_2) - c_6(\dot{y}_3 - \dot{y}_1) \\ \quad -k_4(y_3 - x_4\sin\theta_2 - y_4\cos\theta_2) - k_6(y_3 - y_1) = F_{ex,2} \\ -m_4\ddot{x}_4 + c_4(\dot{y}_3 - \dot{x}_4\sin\theta_2 - \dot{y}_4\cos\theta_2)\sin\theta_2 \\ \quad +k_4(y_3 - x_4\sin\theta_2 - y_4\cos\theta_2)\sin\theta_2 = -F_2\cos\theta_2 - T_2 \\ -m_4\ddot{y}_4 + c_4(\dot{y}_3 - \dot{x}_4\sin\theta_2 - \dot{y}_4\cos\theta_2)\cos\theta_2 \\ \quad +k_4(y_3 - x_4\sin\theta_2 - y_4\cos\theta_2)\cos\theta_2 = F_2\sin\theta_2 - N_2 \end{cases} \tag{2}$$

Internal constraints can be expressed as:

$$\begin{cases} x_1 = x_2\cos\theta_1 - y_2\sin\theta_1 \\ x_3 = x_4\cos\theta_2 - y_4\sin\theta_2 \end{cases} \tag{3}$$

so that the system is reduced to 6 DoFs (y_1, x_2, y_2, y_3, x_4, y_4). To analyze the nonlinear behavior of the system the following status of contact have been considered:

Sticking ($\dot{x}_t = v_p$) ;

Negative Sliding ($\dot{x}_t - v_p < 0$)**:** sliding contact with negative relative speed and positive friction force;

Positive Sliding ($\dot{x}_t - v_p > 0$)**:** sliding contact with positive relative speed and negative friction force;

Detachment ($x_n > 0$)**:** no contact interaction between the mass and the slider.

These conditions can be reached independently on both the contacts between masses and sliders,and the system can reach 4x4 possible combinations of the contact status.

The simulations here reported are performed with the following system parameters where masses are expressed in [kg] and stiffness in [N/m]:

$$\begin{gathered} m_1 = 37.50 \quad m_2 = 0.25 \quad m_3 = 3.75 \quad m_4 = 1.50 \\ k_1 = k_2 = k_3 = \text{2.0e+5} \qquad k_4 = \text{2.3e+5} \quad k_5 = k_6 = \text{2.0e+4}. \\ \mathbf{C} = \beta\mathbf{K} \qquad \beta = \text{5e-5 s} \end{gathered} \tag{4}$$

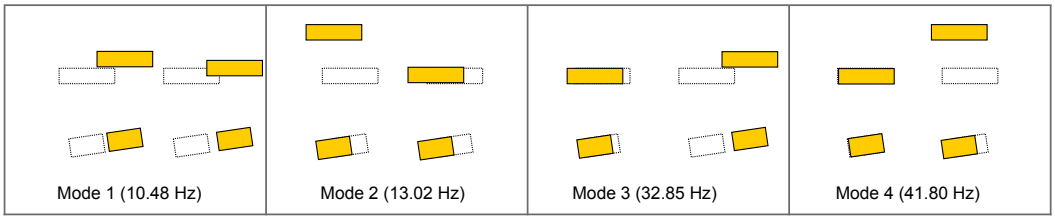

Figure 2: Modal shapes in case of $\mu = 0$.

3 COMPLEX EIGENVALUE ANALYSIS

To find the eigenmodes of the system the equilibrium position is accounted for. It is supposed that all the contacts are in sliding condition. In this case the motion is constrained in the direction witch is normal to the slider. The reaction force N generates a tangential force $\|T\| = \mu N$ whose orientation agrees with that of the rigid slider speed.

In sliding condition the system has 4 DoFs. The Damping matrix is introduced as to be proportional to the stiffness matrix. If the friction coefficient is nil the modes of the system can be expressed solving the eigenvalue problem for the mass and stiffness matrices.

$$\lambda \mathbf{M}\boldsymbol{\Psi} = \mathbf{K}\boldsymbol{\Psi} \tag{5}$$

where $\lambda = \omega^2$ are the real eigenvalues of the system and $\boldsymbol{\Psi}$ are the eigenvector that represent the modal shapes (Fig. 2). The modes at lower frequency correspond to a relevant motion of the left subsystem in vertical direction and to a in phase motion of the two subsystems in horizontal direction while the modes at higher frequency correspond to a relevant motion of only the right subsystem.

If the friction coefficient is different from zero, it produces an asymmetry on the stiffness and damping matrices. The system modes can be found in this case by the means of a complex modal analysis. The system can be expressed in the state space:

$$\begin{cases} \mathbf{M}\ddot{\boldsymbol{x}} + \mathbf{C}\dot{\boldsymbol{x}} + \mathbf{K}\boldsymbol{x} = \boldsymbol{F} \\ \mathbf{M}\dot{\boldsymbol{x}} - \mathbf{M}\dot{\boldsymbol{x}} = \mathbf{0} \end{cases} \tag{6}$$

$$\begin{bmatrix} \mathbf{0} & \mathbf{M} \\ \mathbf{M} & \mathbf{0} \end{bmatrix} \begin{Bmatrix} \dot{\boldsymbol{x}} \\ \ddot{\boldsymbol{x}} \end{Bmatrix} + \begin{bmatrix} \mathbf{K} & \mathbf{C} \\ \mathbf{0} & -\mathbf{M} \end{bmatrix} \begin{Bmatrix} \boldsymbol{x} \\ \dot{\boldsymbol{x}} \end{Bmatrix} = \begin{Bmatrix} \boldsymbol{F} \\ \mathbf{0} \end{Bmatrix} \tag{7}$$

$$\mathbf{A} = \begin{bmatrix} \mathbf{0} & \mathbf{M} \\ \mathbf{M} & \mathbf{0} \end{bmatrix} \qquad \mathbf{B} = \begin{bmatrix} \mathbf{K} & \mathbf{C} \\ \mathbf{0} & -\mathbf{M} \end{bmatrix} \tag{8}$$

$$\lambda \mathbf{A}\boldsymbol{\xi} = -\mathbf{B}\boldsymbol{\xi} \tag{9}$$

where λ are in this case the complex eigenvalues and $\boldsymbol{\xi}$ are the complex eigenvectors of the system. The eigenvalues can be expressed as a function of the angular frequency ω and the damping factor ζ of the mode:

$$\lambda = -\omega\zeta + i\omega\sqrt{1-\zeta^2}. \tag{10}$$

The real part is correlated to the modal damping factor: a positive real part corresponds to modes with apparent negative modal damping factor (unstable modes). When the effects of friction forces increase, eigenvalues have initially different frequency coalesce together (lock-in) and the real parts start to diverge (Hopf bifurcation point).

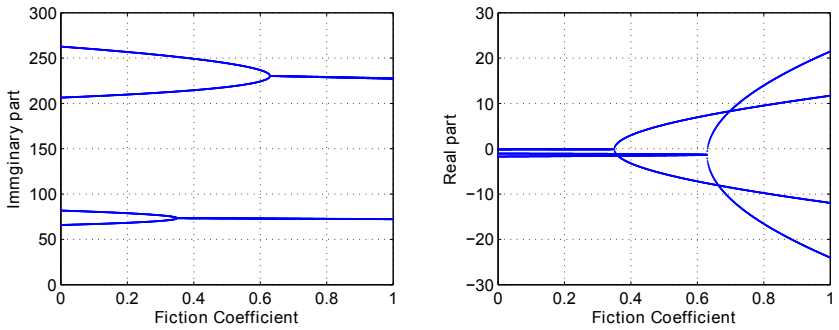

Figure 3: Real and Imaginary part of the eigenvalues versus the friction coefficient

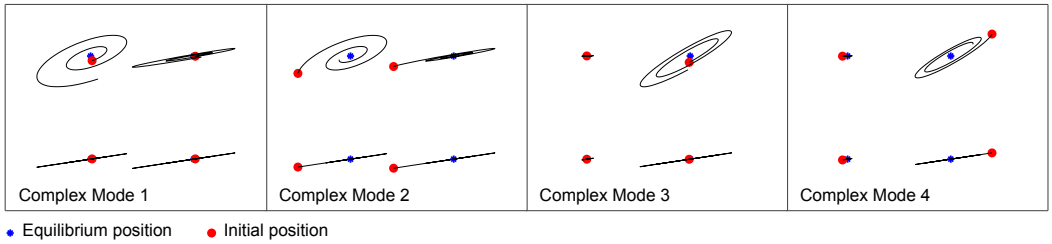

Figure 4: Complex modal shapes for a friction coefficient $\mu = 0.75$

Figure 3 reports the trend of real and imaginary parts of each eigenvalue with respect to the friction coefficient μ. Eigenvalues at lower frequency are the firsts to coalesce for a critical friction coefficient $\mu_I = 0.35$. The two modes at higher frequency coalesce for a friction coefficient $\mu_{II} = 0.63$. It can be noticed that positive real part of the lower eigenvalues overcome the real part of the higher eigenvalue for a friction coefficient between 0.35 and 0.70. The opposite occurs for $\mu > 0.70$.

Complex eigenvectors give information about both the relative amplitude of vibration and the initial phase of the vibration of each degree of freedom. Each pair of complex conjugate modes gives the following (real) contribution to the displacement solution:

$$\boldsymbol{x}(t) = \boldsymbol{\psi}_i \, e^{\lambda_i t} + \boldsymbol{\psi}_i^{\star} \, e^{\lambda_i^{\star} t} = 2 \, \mathrm{Re} \left[\boldsymbol{\psi}_i \, e^{\lambda_i t} \right] \tag{11}$$

The orbits of the masses of the system allow for a physical interpretation of the different eigenvectors both in terms of vibration amplitude and in terms of the phase delay between the different DoFs of the system (Fig. 4). Convergent spirals correspond to stable modes while divergent spiral correspond to unstable modes. For unstable modes the counterclockwise verse produces a variation of the normal and tangential force that agrees with the tangential speed variation giving a power absorption of the system. On the contrary, in stable modes the clockwise verse produces a variation of the contact forces that is in opposition with the tangential speed variation and this gives a power dissipation of the system.

4 TRANSIENT NON LINEAR ANALYSIS

When dealing with linear systems, the solution can be expressed as a linear combination of all the modes of the system. Basing on the real part of the eigenvalues, the system behavior can be stable or

unstable. For linear systems, if there are several unstable modes, the mode with greater real part of the eigenvalues grows exponentially faster than the others, and the contribution of the other modes becomes quickly irrelevant. Real systems don't behave linearly because of the contact nonlinearities that can be the change of contact status (stick, slip, detachment) or the nonlinear contact stiffness. When the vibration amplitude increases, the variation of the contact status (detachment or sticking) confines the exponential growth of the vibration amplitude. This is why the linear model is fully representative only of the initial part of this dynamic instability phenomena. To simulate in a reliable way the whole transient analysis in the case of unstable friction induced vibrations, a non linear model is needed.

In this paper transient analyses have been performed to observe the time evolution of the non-linear system in presence of contact forces considering the nonlinearities introduced by the contact itself. The response of the system has been calculated by a numerical integration of the differential equations of the system starting from an initial condition close to the equilibrium position.

Starting from the contact sliding condition and integrating in time, different scenarios can occurs for each contact pair: i) if the normal contact force reaches the nil value, the mass leaves the slider and pass to the detachment condition; ii) if the relative speed of the mass with respect to the slider reaches the nil value the system can either pass to the sticking status or overcome the nil value with the consequent inversion of relative motion (sign of the friction force).

For each combination of contact status of the contact pairs a different set of differential equations can be written; each time a switch condition is reached, the position in the state plane of the system becomes the initial condition of the new differential set of equations.

4.1 *Effects of friction coefficient on transient behavior.*

With reference to the different behaviors of the system observed by the complex eigenvalue analysis, transient nonlinear simulations have been developed in function of the friction coefficient (see Fig.3):

$\mu < 0.35$**:** the system is stable;

$0.35 < \mu < 0.63$**:** the system is unstable because one of the eigenvalue at lower frequency has a positive real part;

$0.63 < \mu < 0.70$**:** the system is unstable because there are eigenvalues at both lower and higher frequency with positive real part. The real part of the eigenvalue with lower frequency is greater than the other;

$\mu > 0.70$**:** the system is unstable because there are eigenvalues at both lower and higher frequency with positive real part. The real part of the eigenvalue with higher frequency is greater than the other.

In case of stable behavior of the system, the amplitude of vibration decreases with exponential decay factor. If the initial amplitude of vibration is less than the amplitude that brings to the contact status variation, the system behaves linearly and tends exponentially to reach its static equilibrium position.

In case of unstable behavior of the system, the amplitude of vibration, initially induced by a little perturbation, increases exponentially until the first mass reaches one of the possible status variation. Then the exponential increase of the vibration amplitude stops and the system vibrations reaches its limit cycle.

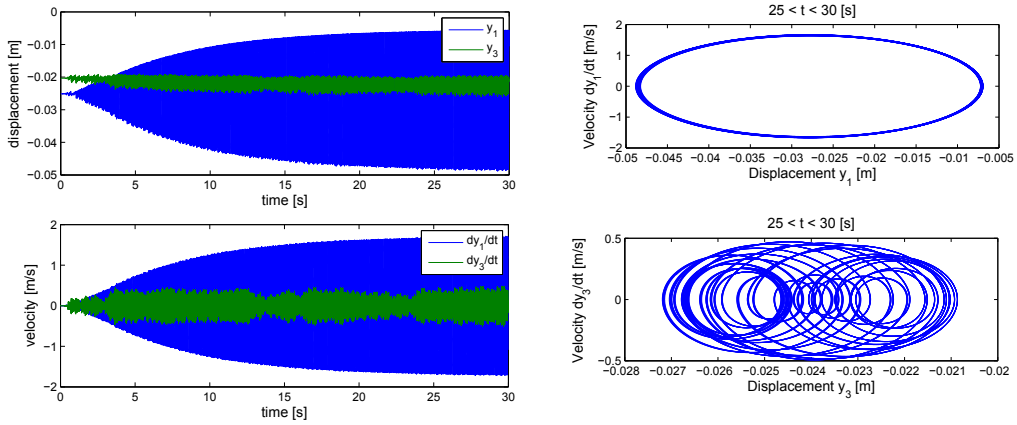

Figure 5: Transient results. $\mu = 0.65$

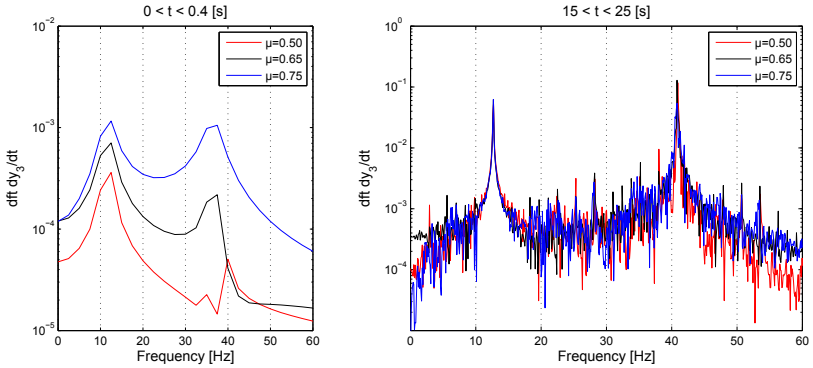

Figure 6: Discrete Fourier Transform of the initial (linear) part and of the final (steady state) part of the system response signal for different friction coefficients

In figure 5, a typical behavior of the system when at least one of the modes is unstable is reported. Results reported in figure 5 are referred to a friction coefficient $\mu = 0.65$. The initial perturbation is $\dot{y}_1(0) = 1e-3\,\mathrm{m/s}$.

The state diagrams of the y_1 and y_3 coordinate highlight the limit cycle of the system. The complexity of the state diagram of the y_3 coordinate is due to the rational ratio $9/29$ between the two frequencies $f_1 = 12.70\,Hz$ and $f_2 = 40.93\,Hz$.

Results of three different analyses with three different values of the friction coefficient and the same initial perturbation are reported in figure 6. The DFT of the system vibrations in the initial part of the simulation show that when the system behaves linearly, the excited frequencies are exactly the same of the complex modal analysis (Fig. 3). Their values increase slightly with the friction coefficient.

In the cases presented in figure 6 the initial perturbation acts on the degree of freedom y_1 and it excites (initially) mainly the first mode at a frequency of about $12\,\mathrm{Hz}$. Increasing the friction coefficient, the peak amplitude corresponding to the second mode (at about $40\,\mathrm{Hz}$) increases faster

than the amplitude of the first mode according to the real part trend of the linear parametric analysis (fig. 3).

Although in the first part of the simulation the system behaves differently for different friction coefficient, due to the different grow rate of the two unstable modes, in the second part of the simulation the limit cycles are very similar in spite of the different value of μ.

The frequencies of vibration calculated by the DFT in this part of simulation are higher than the frequencies calculated during the first (linear) part because of the stiffening of the system due to the presence of sticking motion that acts as a constraint on the direction tangential to the contact.

Furthermore, for increasing friction coefficient the amplitude of vibration of the limit cycle increases slightly. When the friction coefficient is $\mu = 0.50$ the amplitude of displacement oscillation measured on the y_1 direction (see fig. 1) is $\Delta y_1^{50} = 0.0398$; for $\mu = 0.65$ the amplitude of vibration is $\Delta y_1^{65} = 0.0412$ and for $\mu = 0.75$ the amplitude of vibration is $\Delta y_1^{75} = 0.0417$.

4.2 *Effects of the initial condition.*

Figure 7, shows the DFT of the system response for different perturbations (initial conditions), both in amplitude and in shape.

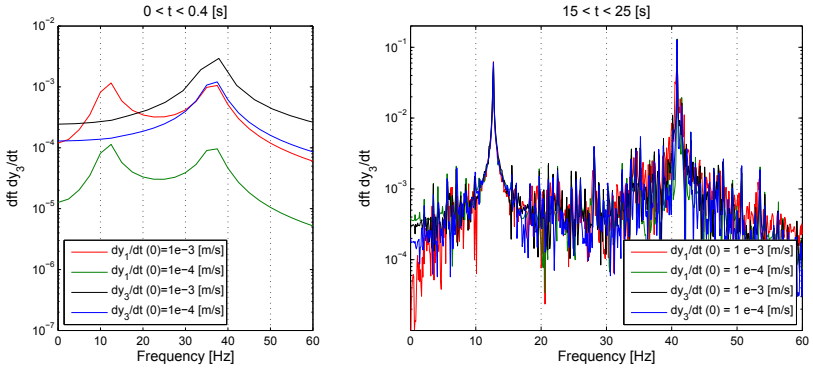

Figure 7: Discrete Fourier Transform of the initial part and of the steady state part of the system response for different initial perturbation.

Result highlighted that different initial perturbations affect only the initial part of the simulation, when the system behaves linearly. The first nonlinearities to appear can also depend on the shape and amplitude of the initial perturbation that may be more similar to an unstable mode rather than to another. In this case, the mode with a shape that is more similar to the initial condition gives to the system response an initial greater contribution. Sometimes if the contact nonlinearities arise when the dynamic of the system is still affected by the initial perturbation, the relative amplitude of the peaks found (in the linear part) do not agree with the real parts of the respective eigenvalues. On the contrary the steady state reached by the system (DFT in the right graph in Fig.7) is not at all affected by the initial perturbation, confirming that the harmonic content and the behavior of the system during the limit cycle is directly correlated to the system parameters.

4.3 *Effects of vertical static load on contact nonlinearities.*

Figure 8 shows the results of three simulations with different external static load F_{ex1} and F_{ex2}. The rest of the system parameters, boundary conditions and initial conditions are kept constant.

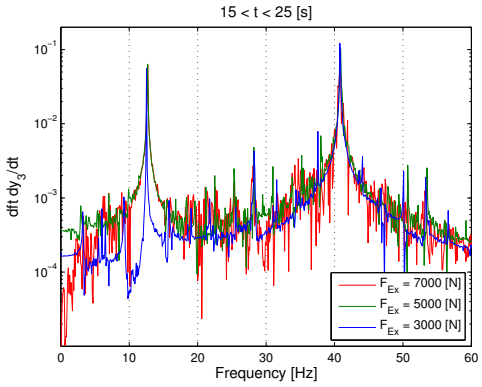

Figure 8: Discrete Fourier Transform of the steady state part of the system response for different external static load.

Friction coefficient for these simulation is $\mu = 0.75$ and the initial perturbation is $\dot{y}_1(0) = 1e-3$ m/s.

One of the main effects of the variation of the external load concerns the amplitude of vibration during the limit cycle. The amplitude variation is strictly related to the periodic switches of the different statuses of the contact pairs.

For high values of preload ($F_{Ex} = 7000\,N$ and $F_{Ex} = 5000\,N$), the contact status alternates between the sticking status and the sliding status (leftmost and central graphs in figure 9) and this corresponds to a very small variation in terms of harmonic content. Horizontal portions of plots dx_2/dt and dx_4/dt indicate a sticking status for the mass m_2 and/or m_4: in this case the dx_2/dt and/or dx_4/dt are equal to the speed of the rigid slider. On the contrary, other portions denote a sliding status. In the leftmost and in the central graph of figure 9 no detachment occurs and dy_2/dt and dy_4/dt are zero.

Reducing the external load ($F_{Ex} = 3000\,N$) some detachments of mass m_2 appear during the limit cycle and are indicated by portions of the plot of dy_2/dt that are different from zero (rightmost graph in figure 9).

In this last case, both the amplitude and the width of the peak at the lower frequency are reduced (figure 8) that means a lower energy content of the system around that frequency.

5 CONCLUSIONS

In this paper, the development and analysis on a lumped parameters non linear model, composed by several degrees of freedom, is presented. The presence of coulombian contact with a constant friction coefficient can make the system unstable. By a parametric Complex Modal Analysis on the linearized model, the effects of the variation of the friction coefficient on the system stability have been highlighted. System configurations with either one or several unstable modes are recovered.

The non linear transient analyses, considering the possibility of the contact status variation at the contact (switching between sliding, sticking or detachment), allow for finding limit cycles of the system by accounting for the contact nonlinearities. The effects of boundary and initial conditions on the initial part (linear) and on the limit cycle (non linear) of the system response have been analyzed.

Results reported in this paper show that when the friction coefficient is in the instability range, variations of the value produce significant variations only in the initial part of the transient simu-

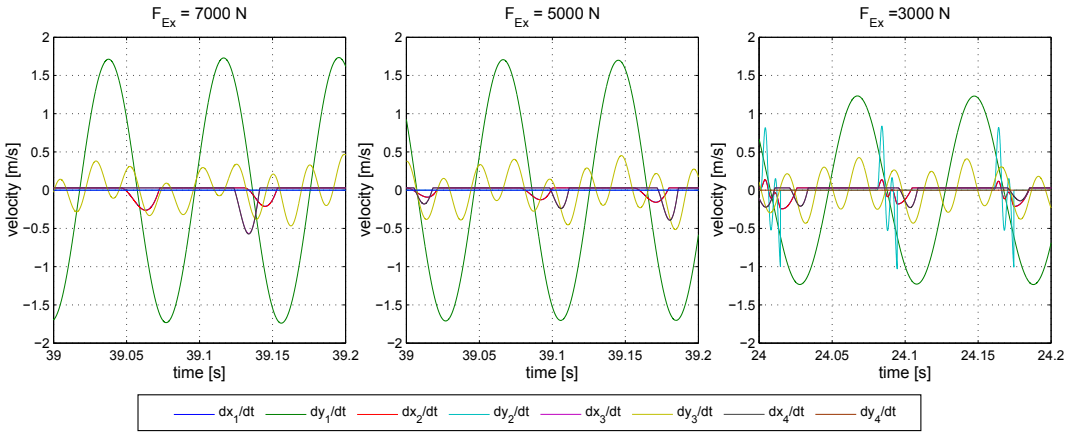

Figure 9: Velocity response during the limit cycle. Graphics from left to right are referred to $F_{ex} = 7000\,\mathrm{N}$, $F_{ex} = 5000\,\mathrm{N}$ and $F_{ex} = 3000\,\mathrm{N}$

lation, where the system behaves linearly and on the beginning of the non linear behavior. In the limit cycle the same harmonic content can be found and only variation of the vibration amplitude are noticed in the case of variation of the friction coefficient.

On the contrary, the external static loads applied to the system modify the contact status during the limit cycle and relevant variations of the harmonic contents can be noticed.

References

[1] Massi, F., Baillet, L. and Culla, A., "Structural modifications for squeal noise reduction: numerical and experimental validation.", *International Journal of Vehicle Design* **51**, 168–189 (2009).

[2] Coudeyras, N., Sinou, J.-J. and Nacivet, S., "A new treatment for predicting the self-excited vibrations of nonlinear systems with frictional interfaces: The Constrained Harmonic Balance Method, with application to disc brake squeal", *Journal of Sound and Vibration* **319**, 1175 – 1199 (2009).

[3] Massi, F., Baillet, L., Giannini, O. and Sestieri, A., "Brake squeal: Linear and nonlinear numerical approaches", *Mechanical Systems and Signal Processing* **21**, 2374 – 2393 (2007).

[4] Sinou, J., Thouverez, F. and Jézéquel, L., "Methods to reduce non-linear mechanical systems for instability computation", *Archives of Computational Methods in Engineering* **11**, 257–344 (2004).

[5] Hoffmann, N. and Gaul, L., "Effects of damping on mode-coupling instability in friction induced oscillations", *ZAMM - Journal of Applied Mathematics and Mechanics / Zeitschrift fur Angewandte Mathematik und Mechanik* **83**, 524–534 (2003).

[6] Tonazzi, D. *et al.*, "Instability scenarios between elastic media under frictional contact", *Mechanical Systems and Signal Processing* – (2013).